ISSN 1392-1207. MECHANIKA. Vol. 29, No. 5, 2023: 350–357

Study on Mechanical Behavior and Deformation Law of Expansion Process of Expansion Screen Base Pipe

Pu LIU*, Zhengqiang TANG*, Ning DAI, Quanlin XIAO*, Zhiping WANG*, Chenlong WANG*****

**College of Mechanical Engineering, Sichuan University of Science & Engineering, Yibin 643002, China, E-mail: 1278908687@qq.com (Corresponding author)*

***PetroChina Offshore Emergency Rescue Response Center, Tangshan 063200, China, E-mail: 207017145@qq.com*

****CNPC Engineering Technology R&D Company Limited, Tianjin 300451, China, E-mail: 486314853@qq.com*

https://doi.org/10.5755/j02.mech.33414

1. Introduction

Expanded tubing technology originated in the 1990s and can be applied in drilling and completion, oil recovery and workover operations, which can solve the borehole redirection problem and significantly reduce operating costs, and is considered one of the core technologies in the oil drilling and recovery industry in the 21st century [1, 2]. Expanded screen pipe technology is an important branch of expanded tubing technology, and the advantages of this technology are [3]: 1. Easy to install, good anti-sand effect and corrosion resistance; 2. Increase the inner diameter of the tubing column, reduce the gap between screen pipe and casing, and reduce the possibility of screen pipe clogging and erosion of broken rings; 3. After expansion, the diameter of screen pipe increases significantly, and the utilization rate of well diameter increases, which is applicable to any type of wellbore; 4. Reduce the skin effect and improve; 5. It can be used to prevent sand in the tubing of lossy wells and effectively solve the problem of serious sand emergence in horizontal wells. Therefore, many scholars have studied the pressure change law, temperature change law, erosion change law and failure change law during the use of expanded screen tubing.

The key factors of affecting sand mesh erosion and the erosion mechanism were analyzed by Abduljabbar in 2022. And experimental results showed the effect of key parameters on screen pipe erosion [4]. The effects of pore size and open flow area on flow and sand control performance are investigated by Roostaei Morteza in 2021, and a comprehensive design process for sand control in cold heavy-oil production (CHOP) in horizontal wells is proposed [5]. The effects of circulating fluid discharge, temperature on response temperature, expansion rate and expansion force were analyzed by Youzhi Duan in 2020 [6, 7]. The structural integrity and slot width variation law of the base pipe of slotted liners were studied by Xiaoda Liu and Nobuo Morita in 2020, and the degree of influence of material grade, casing, tubing size and slot type on the failure risk of slotted liners were analyzed [8]. Zaiming Wang analyzed the feasibility of the screen pipe and performed equal stiffness pipe column crossing before the screen pipe was lowered to achieve the safe lowering of Φ88.9mm sand resistant screen pipe in 2019 [9]. The effects of near-wellbore flow rate, chemical composition of produced water, particle size distribution of formation sand and fines content, and formation clay composition on screen pipe performance were analyzed by Mahmoudi Mahdi in 2018 [10]. The technical advantages of studying inflow control devices with shape-memory polymer conformal screen pipes as an alternative to gravel pack operations were analyzed by Osunjaye Gbenga in 2017 [11]. The relative sand passing volume and calculated circulation performance indexes under different sand control accuracy were analyzed by Changyin Dong in 2016, and an empirical model for optimizing the design of mechanical screen pipe sand control accuracy was established [12]. The reservoir properties of the oil field and the actual production data of the development wells were analyzed by Guangyu Wu in 2015, and the effectiveness of the sand control method was evaluated in terms of sand control effect, skin factor and single well capacity [13]. The scope of application of the expanded screen pipe technology was studied by Ismail I Mohd in 2014, and the performance and reliability of the expanded screen pipe was analyzed [14]. The practical application of expandable screen pipe completion technology was studied by Mason David in 2011, and the impact on well performance in the event of borehole collapse was analyzed [15]. The key technologies of expanded screen pipe such as large diameter expanded screen pipe hangers, expanded threads with slottings and expanded tools were analyzed by Shen Chen in 2011 [16].

In summary, many scholars on the expansion of the screen pipe research mainly focused on the influence of external factors, the expansion process of larger expansion rate to study the mechanical behavior and deformation law research is less.

Expansion screen base pipe should have large deformation capacity and good crack arrest performance, so most of the expansion screen base pipe is made of 316L stainless steel [17]. The expansion process of the expansion screen base is simulated and analyzed by using finite element software ANSYS, in order to obtain the residual stress and shape change of the expansion screen pipe after deformation and to study the deformation and residual stress variation law of the expansion screen pipe at different expansion rates. Provide theoretical basis for onsite construction.

2. Analysis of the mechanical behavior of the expanded screen base pipe

During the expansion of the expanded screen base pipe, the axial force is transformed into the internal pressure of the inner wall of the base pipe through the sloping surface of the expansion cone, and the internal pressure deforms the screen pipe. The deformation process can be divided into

two major processes: shear deformation and bending deformation. When there is less overlap between two slots, the steel bar is subjected to a small bending moment, and its deformation is dominated by shear; when there is more overlap between two slots, the deformation is dominated by bending damage due to the large bending moment, deformation is dominated by bending damage.

2.1. Shear plastic deformation

During the expansion of the expanded screen base pipe, shear deformation and bending deformation occur by axial force, and the gap shape gradually changes from quadrilateral to octagonal [18], as shown in Fig. 1.

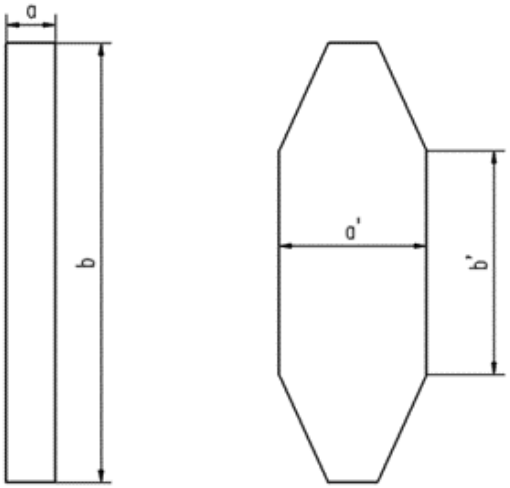

a b

Fig. 1 Schematic diagram of slot deformation: a) before expansion; b) after expansion

Assuming that the node width at the cut joint after expansion remains unchanged, the deformed slot width is shown in Eq. (1).

$$a' = \frac{\pi}{n}\left(D' - D\right) + a, \tag{1}$$

where: a' represents the width of expanded screen base pipe after deformation, a is width of the slot before deformation of the expanded screen base pipe; D' is the external diameter of the expanded screen base pipe after deformation; D is external diameter of the expanded screen base pipe before deformation and n is circumferential slot count.

When there is less overlap between two slots, the steel bar is subjected to a small bending moment, and its deformation is dominated by the shear force, when shear damage occurs, the shear force on a single bar as shown in Eq (2).

$$F_\tau = \tau_S\left(\frac{\pi D}{n} - a\right)t, \tag{2}$$

where: F_τ represents the shear force on steel; τ_s is the shear strength of steel and t represents the base pipe wall thickness.

The pressure that the base pipe can withstand is shown in Eq. (3).

$$P_{ns} = \frac{2\tau_s}{b+c}\left(\frac{\pi D}{n} - a\right)\left(\frac{D}{d} - 1\right), \tag{3}$$

where: P_{ns} represents the n-slot screen pipe shear failure internal pressure; b is the slot length; c is the spacing of peer slots and d is the internal diameter of expanded screen base pipe before deformation.

2.2. Bending deformation

When the two slots overlap more, the deformation is dominated by bending damage due to the larger bending moment of the bar. At this time, the middle part of the overlap-ping bar bending moment is zero, and the two ends are simplified to plastic hinge. The internal pressure is:

$$P_{n\sigma} = \frac{2\sigma_s t}{\left(b^2 - c^2\right)\left(d + t\right)}\left(\frac{\pi D}{n} - a\right)^2, \tag{4}$$

where: $P_{n\sigma}$ represents the n-slot screen pipe bending failure internal pressure; σ_s is the material yield strength.

The actual internal pressure can withstand shear damage and bending damage in the smaller one, then:

$$P = min\left(P_{n\tau}, P_{n\sigma}\right). \tag{5}$$

The axial force on the expanded screen base pipe is:

$$F = \frac{\pi}{4}\frac{sin\theta + cos\theta}{sin\theta\left(cos\theta - fsin\theta\right)}P\left(d'^2 - d^2\right), \tag{6}$$

where: F represents the axial force on the expanded screen base pipe; θ is the expansion cone guide angle; f is the friction coefficient and d' is the internal diameter of expanded screen base pipe after expansion.

3. Finite element equations for the expanded screen base pipe

The basic idea of finite element method is to "break up the whole into parts". The finite element method breaks down a complex structure into relatively simple "units", which are connected to each other by nodes. Based on the elastic-plastic theory of thick-walled cylinder, the finite element equations are established by combining the elastic-plastic deformation mechanism of the base pipe.

3.1. Elastoplastic principal structure relationship of expanded screen base pipe

Expansion screen base pipe expansion process both elastic deformation and plastic deformation, the process is irreversible, according to Von Mises yield criterion, when the external force reaches a certain value, the equivalent stress reaches the material yield limit, under certain deformation conditions, when the elastic properties of the material unit volume shape change (also known as elastic deformation energy) reaches a certain constant, the material is in the form of yield. Therefore, the equivalent stress can be expressed as:

$$\bar{\sigma}=\frac{1}{\sqrt{2}}\left[\left(\sigma_x-\sigma_y\right)^2+\left(\sigma_y-\sigma_z\right)^2+\left(\sigma_z-\sigma_x\right)^2+6\left(\tau_{xy}^2+\tau_{yz}^2+\tau_{zx}^2\right)\right]^{\frac{1}{2}}, \tag{7}$$

where: σ_x, σ_y and σ_z represent the positive stress components in x, y and z directions; τ_{xy}, τ_{yz}, and τ_{zx} represent the tangential stress components in the xy, yz and zx.

After the elastic-plastic deformation of the expanded screen base pipe, the strain increment of the element $\{d\varepsilon\}$ is the sum of the elastic strain increment $\{d\varepsilon^e\}$ and plastic strain increments $\{d\varepsilon^p\}$, i.e.

$$\{d\varepsilon\}=\{d\varepsilon^e\}+\{d\varepsilon^p\}. \tag{8}$$

Due to the generalized Hooke's theorem, the strain increment of the element $\{d\varepsilon\}$ can be expressed as:

$$\{d\varepsilon\}=[D]^{-1}\{d\varepsilon\}+\lambda\left\{\frac{\partial Q}{\partial\sigma}\right\}. \tag{9}$$

Assuming that the material is incompressible, the expansion deformation belongs to the axisymmetric plane state. According to the Prandtl-Reuss equation, the stress-strain increment relationship of the deformation is obtained as:

$$\{d\sigma\}=\left([D]_e-[D]_p\right)\{d\varepsilon\}=[D]_{ep}\{d\varepsilon_p\}. \tag{10}$$

3.2. Elastoplastic principal structure relationship of expanded screen base pipe

In the finite element simulation analysis of the expanded screen base pipe, the load is first divided into several incremental steps, and finally the approximate solution of each quantity is obtained. At each incremental step, the nonlinear equations are approximated as incremental equations, and then the Newton-Raphson method is applied to iteratively solve the displacement, strain, and stress increments at each incremental step to obtain the displacement, strain, and stress at each load step.

Within each load increment step, the elastic-plastic analysis is performed based on the calculated results at the end of the previous increment step. Step m corresponds to load Q_m, step m to step $m+1$ increases load ΔQ, and step $m+1$ corresponds to load $Q_{m+1}(Q_{m+1}=Q_m+\Delta Q)$. Set the displacement u_m, strain ε_m and stress σ_m after step m to increase the load ΔQ. The volume force load, surface force load and displacement boundary conditions of step $m+1$ have an increment, i.e.

$$\begin{cases}\overline{F}_{m+1}=\overline{F}_m+\Delta\overline{F}\left(\text{on the}\,V\right)\\ \overline{T}_{m+1}=\overline{T}_m+\Delta\overline{T}\left(\text{on the}\,S_\sigma\right),\\ \overline{u}_{m+1}=\overline{u}_m+\Delta\overline{u}\left(\text{on the}\,S_u\right)\end{cases} \tag{11}$$

where: $\overline{F}_m$ represents the volumetric force boundary conditions; $\overline{T}_m$ is the external load boundary conditions; $\overline{u}_m$ is the displacement boundary conditions

Then the displacement, strain and stress of step $m+1$ are respectively:

$$\begin{cases}u_{m+1}=u_m+\Delta u\\ \varepsilon_{m+1}=\varepsilon_m+\Delta\varepsilon\\ \sigma_{m+1}=\sigma_m+\Delta\sigma\end{cases}. \tag{12}$$

The equations and boundary conditions they should satisfy are:

Equilibrium equation:

$$A\sigma_m+A\Delta\sigma+\overline{F}_{m+1}=0\left(\text{within V}\right). \tag{13}$$

Geometric equation:

$$\varepsilon_m+\Delta\varepsilon=Lu_m+L\Delta u\left(\text{within V}\right). \tag{14}$$

Constitutive equation:

$$\Delta\sigma=\int_{\varepsilon_m}^{\varepsilon_{m+1}}D_{ep}d\varepsilon=D_{ep}^{\varepsilon'}\Delta\varepsilon\left(\varepsilon_m\le\varepsilon'\le\varepsilon_m+\Delta\varepsilon\right). \tag{15}$$

Boundary equation:

$$\overline{T}_m+\Delta\overline{T}=\overline{T}_{m+1}\left(\text{on the}\,S_\sigma\right), \tag{16}$$

$$\overline{T}_m=n\sigma_m,\Delta\overline{T}_{m+1}=n\Delta\sigma, \tag{17}$$

$$u_m+\Delta u=\overline{u}_m+\Delta\overline{u}\left(\text{on the}\,S_u\right), \tag{18}$$

where: $[D]_e$, $[D]_p$ and $[D]_{ep}$ represent the matrix tensors of elasticity, plasticity and elasto-plasticity of materials

In the elastic-plastic analysis of the expanded screen pipe, D_{ep} is the σ and ε^p function, is linearized and approximated, except for Eq. (16), the rest of the field equations and boundary conditions are linear equations.

4. Finite element simulation analysis of expanded screen base pipe

Using the finite element software ANSYS, numerical simulations are performed for the expansion forming process, which is very complex and involves multiple nonlinearities in geometry, contact, and material. To simplify the calculation, the following assumptions are introduced:

1. Neglecting the energy dissipation due to expansion deformation.

2. Assume that the material is uniformly continuous and isotropic.

3. The contact surface friction coefficient remains constant during the expansion process.

4. Assume that the expansion cone is rigid and does not deform during the expansion process.

4.1. Modeling

The structure of the expansion cone is composed of three parts: guide zone, expansion zone and sizing zone, as shown in Fig. 2. The diameter of the guide zone is 180mm, the cone guide angle is 15°, and the diameter of the

sizing zone is 220 mm, 245 mm, 319 mm and 325 mm according to the specific conditions of an oil and gas well, corresponding to the expansion rate of 20.2%, 33.9%, 74.3% and 77.6% respectively.

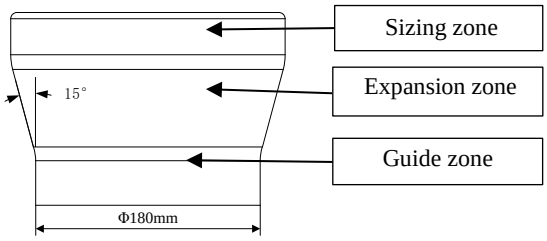

Fig. 2 Schematic diagram of expansion cone

The expansion rate is determined by the size of radial displacement when the expanded screen base pipe expands, and the radial expansion rate should be the same at any point in the axial direction of the base pipe, and the parallel staggered slot and spiral slot can meet the requirements of large deformation rate and equal expansion, but when the spiral slot is used, it is easy to lead to uneven expansion rate of the threaded joint of the screen pipe, so the parallel staggered slot is chosen. Therefore, the base pipe of the expanded screen pipe is adopted as a parallel staggered distribution of rectangular slots, as shown in Fig. 3.

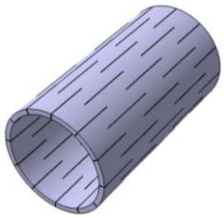

Fig. 3 Expansion screen base pipe number model diagram

Base pipe slot length [19]: L=110 mm, slot width: D=1 mm, evenly spaced angle: α=30°, and detailed dimensions are shown in Table 1.

Table 1

Dimensional parameters of the expanded screen base pipe

External diameter, mm	Wall thickness, mm	Internal diameter, mm	Length, mm	Number of single circumference slots, strip	Slot length, mm	Slot width, mm
203.2	10	183.2	380	12	110	1

4.2. Boundary conditions

In finite element analysis, material parameters have a large impact on the results, so by entering more detailed real mate-rial parameters, the simulation results are closer to the actual situation. By determining the mechanical tensile properties of 316L steel and other related tests, the material property parameters were derived, as shown in Fig. 4, and the resulting data were entered into the mechanical properties of the material through Workbench data.

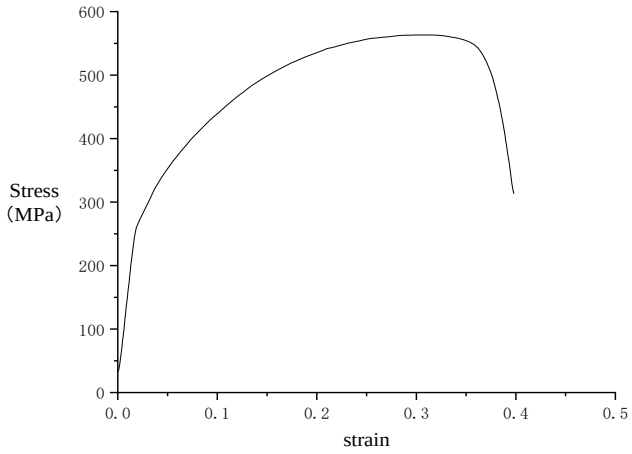

Fig. 4 Stress-strain curve of 316L stainless steel

The expansion cone is set as a rigid body, and the material is set as 42CrMo. The material parameters are shown in Table 2, and its material density, elastic modulus and Pois-son's ratio are input.

Frictional contact is selected between the expansion zone of the expansion cone and the guide zone and the inner sur-face type of the expansion screen pipe, the contact surface and the target are selected as shown in Fig. 5, the friction coefficient is set to 0.1 [1], and the contact algorithm is selected to increase the Lagrangian algorithm.

Table 2

Material parameters of expansion cone and expansion screen base pipe

Designation	Materials	Density, kg/m3	Modulus of elasticity, GPa	Poisson's ratio
Expanded screen base pipe	316L	7980	200	0.3
Expansion cone	42CrMo	7850	203	0.3

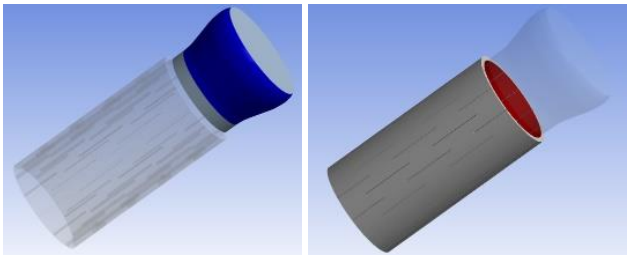

a b

Fig. 5 Target surface and contact surface of expansion screen pipe and expansion cone: a) target surface; b) contact surface

During the analysis, the main focus is on the force and de-formation of the expansion pipe, especially the expansion pipe in the radial deformation, so the expansion pipe in the thickness direction grid encryption. Fig. 6 shows the grid diagram of the expansion screen pipe and expansion cone division. The number and quality of grid cells are shown in Table 3.

According to the actual situation, the boundary conditions are set, and the cylindrical support is applied to the inner surface of the expansion pipe, the axial direction is fixed, the radial direction and circumferential direction are free, and the rest of the surface is not made without any constraint. An axial displacement load is applied to the expansion cone so that the expansion cone passes through the ex-

pansion pipe. Using the Mechanical APDL solver, the expansion process is simulated using the solver command to obtain the expanded expansion screen pipe.

Table 3

Number and mass of cell grids with different expansion rates

Expansion rate	Grid nodes	Grid cells	Average cell mass
20.2	67807	257102	0.79018
33.9	68976	257510	0.80844
74.3	69074	257631	0.80895
77.6	69466	257655	0.80905

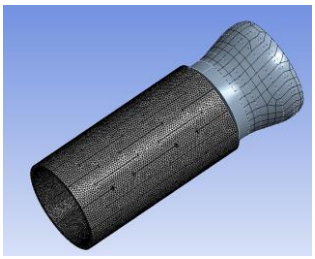

Fig. 6 Finite element mesh diagram of expansion screen pipe and expansion cone

4.3. Simulation results of expanded screen pipe

Numerical simulations of the expansion process were carried out for the expanded screen base pipe at expansion rates of 20.2%, 33.9%, 74.3% and 77.6%, and the wall thick-ness variation curves, radial deformation curves, plastic strain curves, equivalent force clouds, the relationship be-tween the axial thrust required for expansion and the time step and the axial residual stress distribution curves after expansion were obtained for different expansion rates.

1. Wall thickness. The wall thickness variation is an important parameter in the expansion process of the reaction expansion screen base pipe, and its wall thickness variation is shown in Fig. 7.

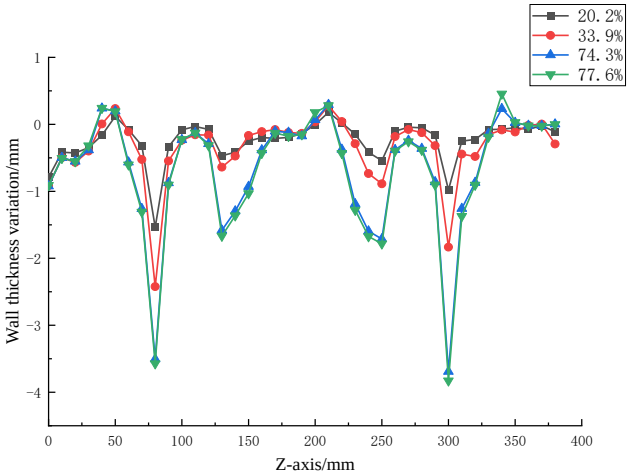

Fig. 7 Wall thickness variation of expanded screen pipe

As can be seen from Fig. 7, the change pattern of the base pipe under different expansion rates is the same, the wall thickness increases in the middle position of the slot and thins at both ends, and the wall thickness increases by the same size, the maximum increase of 0.28 mm; the thinning amount of different degrees of expansion is different, and the reduction is proportional to the expansion rate, in which 20.2% of the wall thickness decreases by 1.5 mm, and the expansion rate is 77.6% of the wall thickness decreases by 3.8 mm. indicating that in the expansion process During the expansion process, the middle region of the slot was subjected to the equivalent of extrusion stress and the material rebounded.

2. Radial deformation. The size of radial deformation can visually reflect the deformation of the expanded screen base pipe. The deformation of the slot in the expansion process consists of two parts: plastic deformation and elastic deformation. The elastic deformation region in the expansion process will produce a part near its growth in the opposite direction at the end of the process. After the expansion deformation, the axial change of its radius is shown in Fig. 8, and the total deformation cloud of the expanded screen base pipe is shown in Fig. 9.

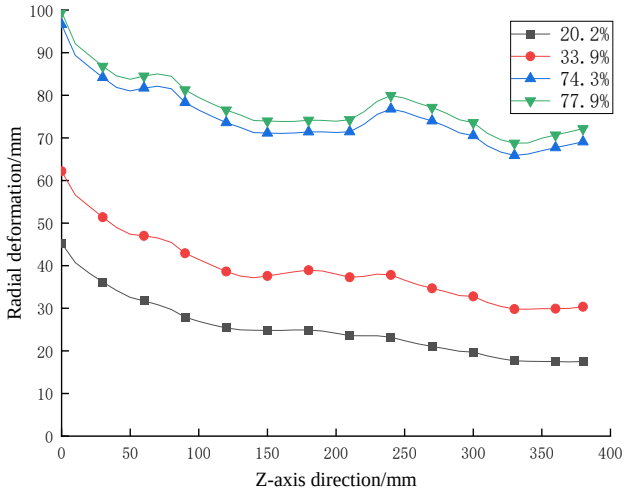

Fig. 8 Axial deformation diagram of the expanded screen base pipe

Comprehensive Fig. 8 and Fig. 9 can be seen that the deformation law of different expansion rates is consistent. The amount of deformation gradually decreases with the axial direction, at the inlet end of the expansion cone, the expansion of the expansion screen base pipe deformation is the largest, exceeding the preset expansion rate, the preset expansion of 20.2%, the simulation result is 45.28 mm, an additional expansion of 29.2%; preset expansion of 77.6%, the simulation result is 99.587 mm additional expansion of 31%. At the outlet end of the expansion cone, the expansion deformation of the expansion screen base pipe is slightly less than the preset expansion rate, the preset expansion of 20.2%, the simulation result is 18.14 mm, a reduction of 0.4%; preset expansion of 77.6%, the simulation result is 68.686 mm reduction of 1.6%.

3. Axial force. Axial force is the power required for the axial movement of the expansion cone during the expansion operation of the screen pipe, and is one of the important parameters for the evaluation of the construction operation of the expanded screen pipe. The curve of the axial thrust force required during the expansion of the base pipe with the time step is shown in Fig. 10.

From the Fig 10. it can be seen that the axial force before the contact between the expansion cone and the base tube of the expansion screen pipe is 0. After the expansion starts, the contact area between the base pipe and the expansion cone increases, resulting in an increase in the axial

force. A certain oscillation situation in the middle curve indicates that the expansion cone finishes entering the base pipe, and with the complete expansion of the plastic hinge region, the axial force starts to drop, and when the expansion reaches the midpoint of the first slot, the axial force reaches the first lower stop, after which, it starts to enter the next plastic hinge region and the axial thrust increases again. The expansion cone is moved out from inside the base pipe, and the axial force decreases rapidly until the expansion cone is completely moved out, the axial force becomes 0, and the expansion is completed.

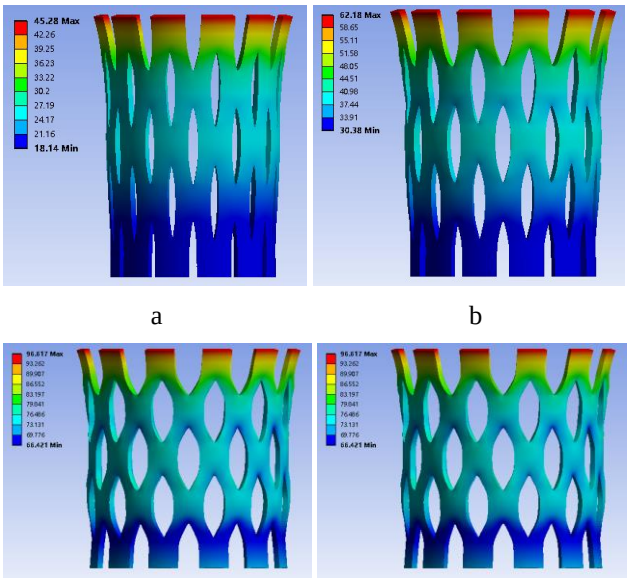

Fig. 9 Total deformation cloud of expanded screen pipe: a) expansion rate of 20.2%; b) expansion rate of 33.9%; c) expansion rate of 74.3%; d) expansion rate of 77.6%

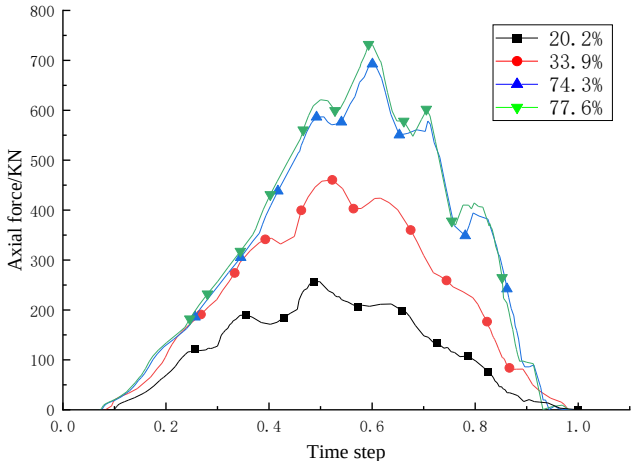

Fig. 10 Total deformation cloud of expanded screen pipe

The maximum axial force required for the expanded screen base pipe increases with the expansion rate. The maximum axial force is 257.8 kN for 20.2% expansion rate, 460.4 kN for 33.9%, 692.57 kN for 74.3% and 732.1 kN for 77.6%.

4. Residual stress. The expansion process of the expanded screen pipe is geometric deformation and plastic deformation of two parts, its yield criterion obeys Von Mises yield criterion, so after expansion, considering the friction effect, the applied expansion stress is divided into the stress released by the geometric deformation and plastic deformation of the base pipe material, by the friction effect into heat energy and stored in the internal stress of the base pipe material and other parts. According to the fourth strength theory of material, the equivalent stress can be directly used in the base pipe strength analysis. Fig. 11 shows the equivalent stress after the expansion of the expanded screen base pipe.

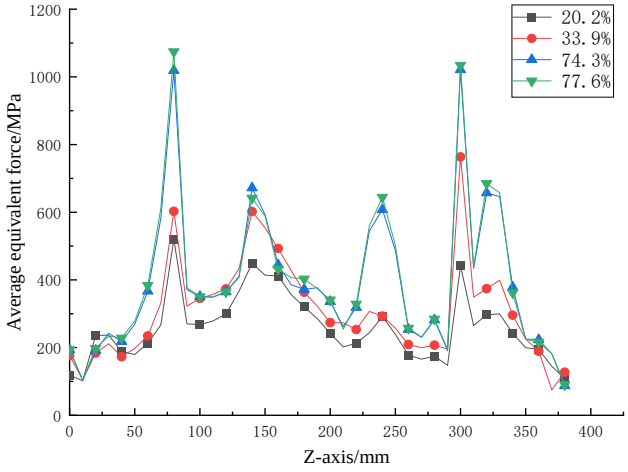

Fig. 11 Total deformation cloud of expanded screen tube

As can be seen in Fig. 11, the distribution of tubular residual stresses is almost the same except for the ends of the slot. The larger the expansion rate is, the higher the residual stresses at both ends of the slot. During the expansion process, when the equivalent stress first increases to the maxi-mum value, the slot starts to deform and causes the equivalent stress to be released when the equivalent stress cannot be increased, while keeping the equivalent maximum stress constant. Fig. 12 shows the equivalent stress cloud of the expanded screen base tube after expansion.

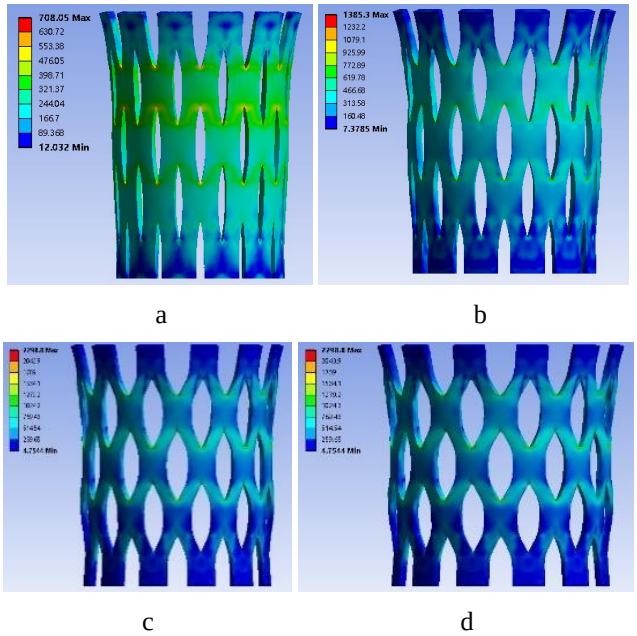

Fig. 12 Equivalent force cloud of expanded sieve tube: a) expansion rate of 20.2%; b) expansion rate of 33.9%; c) expansion rate of 74.3%; d) expansion rate of 77.6%

The residual stress after the expansion of the base

pipe is the residue of the internal equivalent force, which is actually caused by the uneven deformation during the expansion process. It can be seen from Fig. 12 that the distribution of tubular residual stresses is almost the same except for the two ends of the slot, and the maximum value of residual stresses for different expansion rates is proportional to the expansion rate. During the deformation of the expandable screen, the deformation is not uniform throughout due to the slot. The deformation at the end of the slot is larger, so the wall thickness changes a lot, but the wall thickness of the middle part of the slot increases slightly, that is, the slot can provide the tip plastic deformation area, which causes the slot to expand laterally, thus achieving the tubular radial expansion.

5. Equivalent plastic deformation. Equivalent plastic strain is a physical quantity used to determine the location of the yield surface of a material after strengthening, which can objectively reflect the degree of internal deformation of the object. The axial distribution of equivalent plastic strain is shown in Fig. 13.

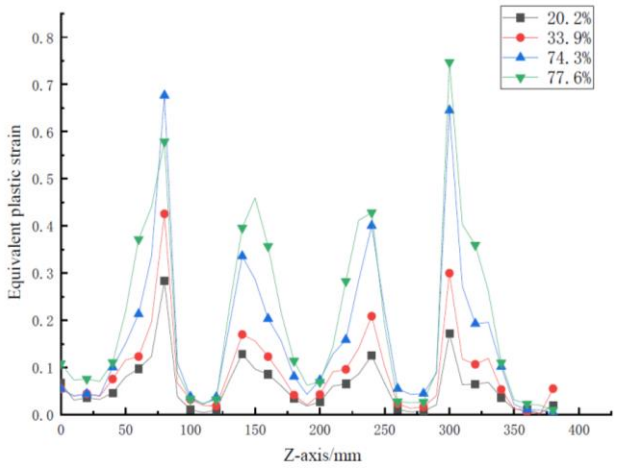

Fig. 13 Equivalent force cloud of expanded screen pipe

From Fig. 13, it can be seen that the expanded screen base pipe is not uniform, with the largest deformation at the end of the slot and the smallest deformation at the middle of the slot. The plastic deformation at the end of the slot is proportional to the expansion rate, and the plastic deformation at the remaining positions is not related to the expansion rate. The maximum equivalent plastic strain in all expansion rates is 0.75, which is much smaller than the actual deformation of the expanded screen base pipe, indicating that the deformation of the expanded screen base pipe is dominated by geometric deformation.

5. Conclusion

Based on the elastic-plastic mechanical analysis of the expansion process of the expandable screen pipe, a nonlinear finite element analysis model of the contact process was established. For the 316L stainless steel screen pipe of 203.2 mm, the expansion deformation process was simulated in the range of 20.2-76.6% expansion rate at room temperature. The conclusions are as follows.

1. Expansion rate has no effect on the increase in wall thickness, which does not change with the expansion rate, the maximum increase of 0.28 mm; the reduction is proportional to the expansion rate, 20.2% of the maximum reduction in wall thickness of 1.5mm, the expansion rate of 77.6% of the maximum reduction in wall thickness of 3.8 mm.

2. At the inlet end of the expansion cone, the expansion screen base pipe expansion deformation is the largest, will be additional expansion of about 30%, the export end expansion rate than the preset expansion rate of about 1% smaller.

3. The residual stress distribution is not uniform, and the residual stress distribution along the slot is cyclic. The maximum residual stress appears at the intersection of the slot tip and the slot opening deformation, and the maximum stress value is proportional to the expansion rate, while the stress value at the remaining locations is significantly lower.

4. The maximum axial force required for the expanded screen base pipe increases with the expansion rate. The maximum axial force is 257.8 kN for 20.2% expansion rate, 460.4 kN for 33.9%, 692.57 kN for 74.3% and 732.1 kN for 77.6%.

5. The expansion deformation of the expanded screen pipe is dominated by geometric deformation, the plastic deformation is relatively small and uneven, the plastic de-formation at the end of the slot is proportional to the expansion rate, and the plastic deformation at the rest of the position is not related to the expansion rate.

6. Acknowledgments

This work is supported by The Project of Sichuan University of Science & Engineering (No. 2020RC18) and The Key Project of Sichuan Provincial Key Lab of Process Equipment and Control (No. GK202007). We gratefully acknowledge the financial support received.

References

1. **Zhu, H. B.; Yu, Z. S.; Tang, C.L.;** et al. 2012. Optimization of expansion parameters and expansion simulation of expansion pipes, Journal of Xi'an Jiaotong University 46(01): 103-107 (in Chinese).
2. **Xu, H; Xia, W.A.; Zhang J. T.;** et al. 2013. Application of expansion pipe technology in T816KCH2 well in Tahe oilfield, Special Oil and Gas Reservoirs 20(05): 145-147 (in Chinese). http://dx.doi.org/10.3969/j.issn.1006-6535.2013.05.034.
3. **Ning, X. T., Wu, L. G.; Tang, C. L.;** et al. 2012. Study on the threaded connection technology of expanded screen pipe, China Petroleum Machinery 40(04): 42-45 (in Chinese). http://dx.doi.org/10.16082/j.cnki.issn.1001-4578.2012.04.019.
4. **Abduljabbar, A.; Mohyaldinn, M. E.; Younis, O.;** et al. 2022. Erosion of sand screens by solid particles: a review of experimental investigations, Journal of Petroleum Exploration and Production Technology 12(8): 2329-2345. http://dx.doi.org/10.1007/s13202-022-01467-4.
5. **Roostaei, M.; Cespedes, E. A. M.; Uzcátegui, A. A.;** et al. 2021. Optimization of slotted liner in rubiales field: trade-off between sand control, flow performance, and plugging tendency, SPE Journal 26(03): 1110-1130. http://dx.doi.org/10.2118/199062-PA.
6. **Duan, Y. Z.; Ai, S.; Liu, H. L.;** et al. 2019. Shape-

memory screen pipe self-filling sand prevention completion technology, Petroleum Drilling Techniques 47(5): 86-90 (in Chinese).
http://dx.doi.org/10.11911/syztjs.2019106.

7. **Duan, Y. Z.; Liu, H. L.; Ai, S.;** et al. 2020. Testing the expansion performance of shape memory screen pipe, Petroleum Drilling Technology 48(04): 83-88 (in Chinese).
http://dx.doi.org/10.11911/syztjs.2020038.
8. **Liu, X. D.; Morita, N.** 2020. Collapse and bending analysis of slotted liners with laboratory tests and 3D FEM, SPE Journal 25(05): 2353-2372.
http://dx.doi.org/10.2118/191441-PA.
9. **Wang, Z. M.; Shen, Y. Y.; Li, Y. F.;** et al. 2019. Φ139.7 mm small borehole sidetrack top cementing process in well G104-5P54CP1, Drilling & Production Technology 42(06): 116-118 (in Chinese).
http://dx.doi.org/10.3969/J. ISSN.1006-768X. 2019. 06. 33.
10. **Mahmoudi, M.; Fattahpour, V.; Velayati, A.;** et al. 2018. Risk assessment in sand control selection: introducing a traffic light system in stand-alone screen selection, SPE International Heavy Oil Conference and Exhibition 2018D32S-D41S.
http://dx.doi.org/10.2118/193697-MS.
11. **Osunjaye, G.; Abdelfattah, T.** 2017. Open hole sand control optimization using shape memory polymer conformable screen with inflow control application, SPE Middle East Oil & Gas Show and Conference 2017D31S-D33S.
http://dx.doi.org/10.2118/183947-MS.
12. **Dong, C. Y.; Zhang, Q. H.; Gao, K. G.;** et al. 2016. Screen sand retaining precision optimization experiment and a new empirical design model, Petroleum Exploration & Development 43(6): 1082-1088.
http://dx.doi.org/ 10.11698/PED.2016.06.17.
13. **Wu, G. Y.; Cao, Y. F.; Shi, D. P.** 2015. Sand control practice in West African deepwater A oil field, Oil Drilling & Production Technology 37(01): 121-123 (in Chinese).
http://dx.doi.org/10.13639/j.odpt.2015.01.031.
14. **Ismail, I. M.; Geddes, M. W.** 2014. Fifteen years of expandable-sand-screen performance and reliability, Spe Drilling & Completion 29(02): 141-149.
http://dx.doi.org/10.2118/166425-PA.
15. **Mason, D.; Benaichaoui, F.; John, H.;** et al. 2011. Expandable completion liners: a comparison of performance with other completion types in the reg and teguentour fields, Algeria, SPE Drilling & Completion 26(2): 255-267.
http://dx.doi.org/10.2118/132692-PA.
16. **Shen, C.; Ning, X. T.; Zhu, H. B.;** et al. 2011. Research on sand control technology of expanded screen pipe, Oil Drilling & Production Technology 33(01): 102-104.
http://dx.doi.org/10.13639/j.odpt.2011.01.027.
17. **Shen, W. Z.; Li, C. F.; Song, K. H.;** et al. 2011. Finite element simulation of deformation process of 316L expandable slotted base pipe at room temperature, Advanced Materials Research 402: 719-723.
http://dx.doi.org/10.4028/www.scientific.net/ AMR.402. 719.
18. **Li, Z. F.; Li, J. Y.; Zhao, P.;** et al. 2003. Mechanical analysis of expanded screen pipes. China Petroleum Machinery 31(12): 6-8 (in Chinese).
19. **He, Y.R; Zhu, H.B.** 2011. Development and field test of expanded screen pipe, Petroleum Drilling Techniques 39(03): 106-109 (in Chinese).
http://dx.doi.org/10.3969/j.issn.1001-0890.2011.03.020.

P. Liu, Z. Tang, N. Dai, Q. Xiao, Z. Wang, C. Wang

STUDY ON MECHANICAL BEHAVIOR AND DEFORMATION LAW OF EXPANSION PROCESS OF EXPANSION SCREEN BASE PIPE

S u m m a r y

The expansion process of the base pipe of the expanded screen pipe includes large displacement elastic-plastic deformation problems such as geometric nonlinearity, material nonlinearity and contact nonlinearity. In this paper, based on the elastic-plastic deformation mechanism of the base pipe of expanded screen pipe, finite element equations are established and numerical simulation is used to construct a finite element simulation model to study the mechanical behavior and deformation law of Φ203.2 mm base pipe of the expanded screen pipe expansion process. The results show that the expansion rate has no effect on the increase of wall thickness, and the decrease is proportional to the expansion rate. The greater the expansion rate, the greater the residual stress at both ends of the slot.

Keywords: expandable screen, the base pipe, finite element analysis, nonlinearity.

Received February 18, 2023
Accepted October 9, 2023